

## Gunn Oscillations in Planar Heterostructure Devices

**A. Kahlid, M. C. Holland, C. R. Stanley, I. G. Thayne, D. S. R. Cumming**  
*Department of Electronic and Electrical Engineering, University of Glasgow,  
Glasgow G12 8LT, United Kingdom*

**N. Pilgrim, G. Dunn**  
School of Engineering and Physical Sciences, University of Aberdeen,  
Aberdeen AB24 SFX, United Kingdom

### Abstract

*Planar Gunn oscillation sources, which offer the prospect of THz operation and increased ease of integration over more traditional vertical structures have been modelled and experimentally realized. The material used was grown by MBE and the devices were made using electron beam lithography. So far, both diode and triode devices capable of from 30 to 108 GHz have been successfully realized.*

### 1 Introduction

Gunn diodes are normally constructed in a "vertical" configuration, with contacts to the top and bottom of the semiconductor layers. The joule heating of these structures gives rise to a key limitation of this geometry, namely that in most cases electron densities much greater than  $10^{16}$  cm<sup>-3</sup> are not possible. This sets a lower limit of about 1.3 microns to the device length, since the density determines the Gunn domain size and a thus sets the minimum length below which a domain will not have room to form and transfer. An upper frequency limit of about 90 GHz for fundamental mode operation is therefore imposed on these devices and even this is by no means easy to achieve. In fact, the A notable planar design, however, is the Field Effect Controlled Transferred Electron Device "FECTED" of Thim and Kuch [3-5], designed to operate in transit time independent mode by exploiting the negative differential resistivity (NDR) of a domain trapped under the gate of the device. Other authors have at various times commented on the possibility of Gunn instabilities forming in FET and HEMT structures [6,7] though this idea has not become established and can still inspire

majority of vertical devices are constructed to be a little longer and designed to operate at about half this frequency, with power being extracted by second harmonic operation. Such devices require further expensive processing to integrate them into a complete oscillation system or with planar integrated circuits, all of which cause unwelcome additional costs. It is for this reason that the possibility of horizontal (planar) device architectures has been explored, such a configuration being particularly well suited to monolithic integration. Historically such explorations have been largely unsuccessful, this being attributed to growth and fabrication issues such as high impurity or trap densities [1-2].

lively debate at conferences. Furthermore, recently a number of papers [8] have concluded that the well-known "kink effect" in HEMTs [9] could be explained by the presence of Gunn domains, these causing the sudden drop in drain current at certain points in the IV characteristics.

Beyond the improved opportunities for device integration, planar structures also have the potential for higher frequency operation. This property is derived from

their ability to maintain high charge densities, much as may be observed in devices. Such densities permit the formation of narrower domains, shorter transit regions therefore become possible and consequently, operation at higher frequencies is achievable.

Finally, it is important to note that in vertical structures the frequency of operation is largely set during growth, by the selection of a particular semiconductor epilayer thickness for the whole or part of the device height. Planar devices, as discussed here, have an advantage in that the frequency of operation is defined by the metal contact separation. This can allow one particular wafer to be used in the fabrication of structures of different frequencies, perhaps even on the same chip.

In this paper we will present the results of our investigations into HEMT like diode and triode structures which behave as high frequency Gunn oscillators. In section 2, the theoretical and experimental methods will be discussed, whilst in section 3 our results will be presented and our conclusions will be summarised in section 4.

**2.1 Simulation Methodology** The chosen modelling technique for the investigation of these structures is the Monte Carlo (MC) method, an approach with a great degree of pedigree for investigative semiconductor device modelling. While computationally not the most rapid of models, its flexibility, accuracy and its ability to extract a wide range of physical parameters concerning the simulated designs are significant advantages over more conventional models. External contact currents are sampled as a function of time, but internal maps of electron density, electric field and many other properties may also be obtained.

The computational engine at the heart of the MC model used here, treats each semiconductor material in a unipolar manner with three analytical electron

other planar heterostructure

bands, with the electron-phonon and ionised-impurity interactions treated as scattering processes in the usual way (Fermi Golden Rule). Repeated solution of the Poisson equation, taking into account fixed (dopant) and mobile charges, ensures that electronic self-consistency is maintained. A representative electron population composed of "super-particles" migrates through the device geometry and across heterolayers, according to the local electric fields calculated from the Poisson equation solutions. Contacts are modelled in the standard MC way, with the annealing present in the devices under investigation here approximated by a highly-doped region of GaAs directly under the contact location and surface charge densities are assumed to create the correct potential boundary conditions.

Approximately 30,000 electron particles are used in each simulation with a field adjusting time-step of 5fs. Here, results are reported for simulations both with and without an assumed sinusoidal RF feedback in order to simulate the behaviour of devices in an appropriate cavity. Figure 1 shows a typical simulated structure with the details of the layer structure investigated given in the next section.

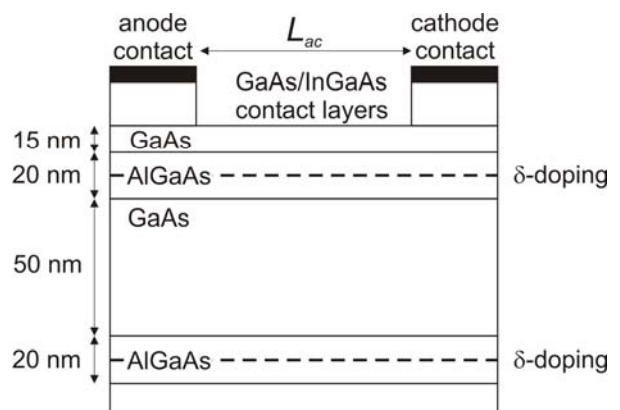


**Figure 1:** The layer structure of the planar Gunn diode showing the recess etch between the contacts.

**2.2 Experimental Methodology** The semiconductor material was grown by

molecular beam epitaxy (MBE) to match the layer properties specified by device modelling. The surface layer is 15 nm of highly doped n-GaAs followed by 20 nm of undoped  $\text{Al}_{0.23}\text{Ga}_{0.77}\text{As}$  layers with  $\delta$ -doping in the middle with an areal density of  $8 \times 10^{11} \text{ cm}^{-2}$ . The channel layer is 50 nm of GaAs. Beneath the channel layer there is a further 20 nm thick AlGaAs layer that is also  $\delta$ -doped. The channel layer is estimated to have an electron charge density of  $\sim 10^{17} \text{ cm}^{-3}$ . Multiple graded layers of GaAs/InGaAs layers are grown above the device active regions in order to aid the formation of Ohmic contacts. These layers are subsequently removed from the active device area as described below.

The as-grown wafers were cleaved into 15 mm x 15 mm samples. Device mesas were made by electron beam direct write into UV-III resist and etching in 1:1:10 of  $\text{H}_2\text{O}_2:\text{H}_2\text{O}:\text{H}_2\text{SO}_4$  solution for 90 s at an etch rate of 60 nm/s. Ohmic contact patterns were made by electron beam direct write into a bilayer of poly methyl(methacrylate) (PMMA) resist (high molecular weight on top of low molecular weight). Prior to contact metal deposition, the patterned sample was oxygen plasma cleaned using 100 W for 60 s. The contact areas were then de-oxidised in 1:4  $\text{HCl}:\text{H}_2\text{O}$  for 30 s followed by 1:10  $\text{NH}_4\text{OH}:\text{H}_2\text{O}$  for 30 sec.

The sample was then rinsed in water before drying. N-type contacts were made by sequential deposition of 20 nm Pd, 50 nm Ge, 10 nm Au, 50 nm Pd and 150 nm Au. The final layer of gold helps to give a surface suitable for device probing. After lift-off, the samples were annealed at 400 °C for 60 s in an optically heated rapid thermal annealer. The typical contact resistivity after processing was  $5 \times 10^{-6} \Omega\text{-cm}^2$ .

The final step in the fabrication of the devices was the removal of the unwanted GaAs/InGaAs contact layers above the active region. This was facilitated using an

$\text{Al}_{0.8}\text{Ga}_{0.2}\text{As}$  etch stop layer that was inserted during wafer growth [10]. The samples were etched in 3:1 citric acid: $\text{H}_2\text{O}_2$  (50% w/w citric acid) solution for 20 seconds. Figure 2 shows an optical micrograph of a completed device.

Since the Ohmic contact separation is controlled by the lithographic dimensions we are able, within the limits of process tolerance, to choose the anode-cathode distance ( $L_{ac}$ ), and hence the electron transit distance.

Prior to making RF measurements, each of the diodes is probed at DC to evaluate their current-voltage (*IV*) characteristics. The data was taken using a combined DC and pulsed *IV* measurement system (DIVA D210) in order to observe and compare the effect of Joule heating on the device. The measurement system used for radio frequency (RF) measurements is shown schematically in Figure 2.

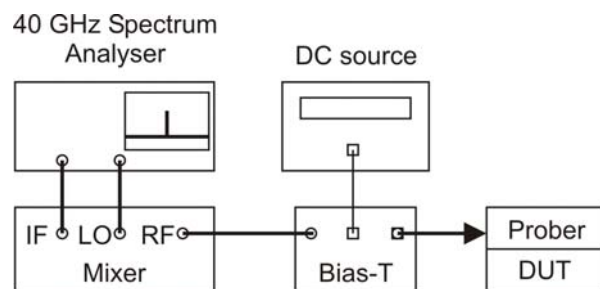


**Figure 2:** The setup for measuring the RF output from the devices using a W-band GSG probe.

The experimental set-up uses a 40 GHz spectrum analyser, the operating range of which has been extended to the W-band using an external mixer. The intermediate frequency (IF) of the mixer is connected to the RF input of the spectrum analyser. The local oscillator (LO) frequency is in the range 2.9 GHz to 6.6 GHz, and it is from a generator built into the spectrum analyser.

### 3 Results & Discussion

**3.1 Simulation** Our simulations have shown that the ability of these structures to

sustain Gunn oscillations is critically dependent on the lateral potential profile across the device (from the surface going down). The ideal state for Gunn domain operation in these structures occurs when the electrostatic potential across the *active* device layers (the channel and layers immediately adjacent to the channel) is essentially flat. In this situation the top device surface layer(s) need to be depleted by the surface charge as near completely as can be managed. This is necessary so that a parallel conduction channel can not be set up along the bottom of the surface layer (effectively short circuiting the Gunn effect) or the electron density in the channel becomes too depleted (effectively preventing domain formation).

Once the above surface depletion conditions have been met, simulations of both diode and triode structures, based on the same layer sequence, show the formation and evolution of Gunn dipoles. The triode structure does however show the most promise. In this structure, the dipole is found to form exactly at the gate, whereas the position of formation in the diode is more nebulous leading to a less well defined natural frequency. The triode structure also offers the possibility of electronic tuning through the gate as the depletion around the gate controls the exact location of the domain formation and hence its frequency. Figure 3 shows a typical Gunn domain transfer in a triode structure.

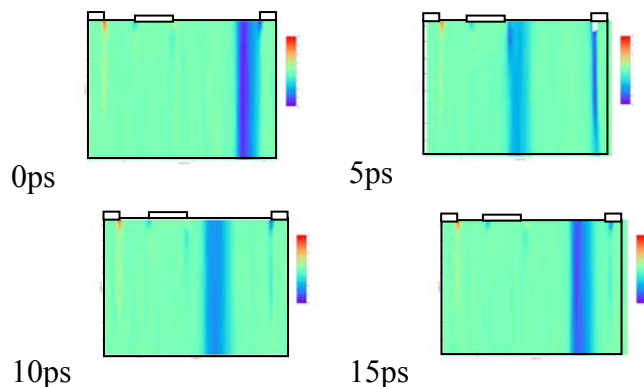


**Figure 3:** Transfer of a Gunn domain in a

triode structure (darker grey indicates higher electric field).

Simulations of a 3  $\mu\text{m}$  diode structure with an RF feedback potential are shown in figure 4 using an artificially-applied 1.6V AC bias over a 4V DC level. At 300K, the natural frequency of a Gunn domain transit is found to be between 37-40GHz at a constant 4V DC bias. If it is assumed that the domain transit speed is  $10^5$  m/s then this translates to a transit distance of 2.5-2.7 $\mu\text{m}$  which corresponds to a dead space in this device of  $\sim 0.3$ -0.5 $\mu\text{m}$ . Figure 4, however, for the device response with the RF feedback potential, has peaks at 300K and 400K of around 33-34GHz. As usual, these frequencies are marginally lower than those from application of a constant DC bias, with higher temperatures corresponding to a lower relative power output.

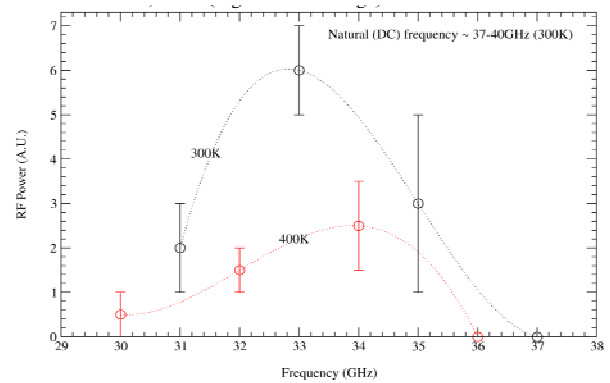


**Figure 4:** RF power calculated for a 3 $\mu\text{m}$  planar Gunn diode.

**3.2 Experimental** The results in this paper are for a devices with a  $L_{ac}$  of 1.3  $\mu\text{m}$  to 3  $\mu\text{m}$  and typical device widths of 60  $\mu\text{m}$ .

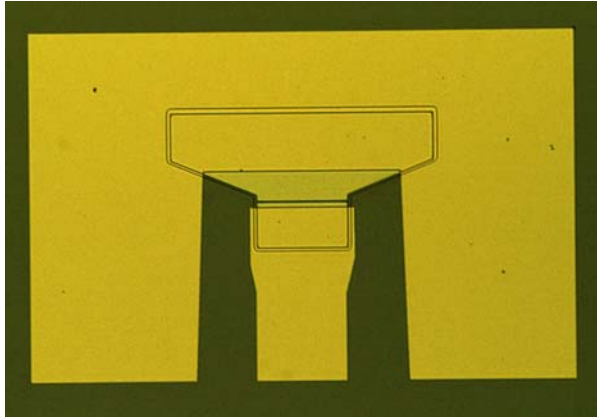


**Figure 5:** An optical micrograph of a completed device (diode).

We do however expect that the effective  $L_{ac}$  will be slightly shorter due to some lateral diffusion during the contact anneal. Figure 5 shows an optical micrograph of a typical completed device (diode) and figure 6 shows a typical  $IV$  plot for one of the devices.

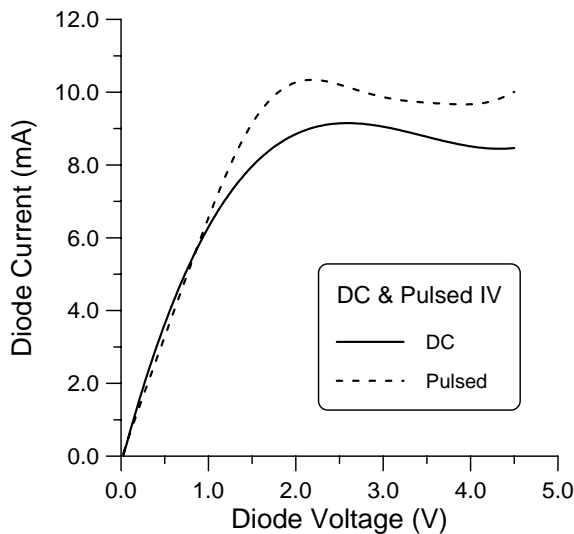


**Figure 6:** Current-voltage characteristics of a planar Gunn diode with 1.3  $\mu\text{m}$  anode cathode separation. The device width is 60  $\mu\text{m}$ .

We find that the result is highly reproducible. The devices are generally found to be more conductive under circumstances of pulsed stimulus (see figure 6) and there is a negative differential resistance region in the device. The current in the device reaches 10 mA which is equivalent to 1.66 A/mm. These results

are comparable to theoretical data from Monte Carlo simulations that we have performed, and the prior art [8][11].

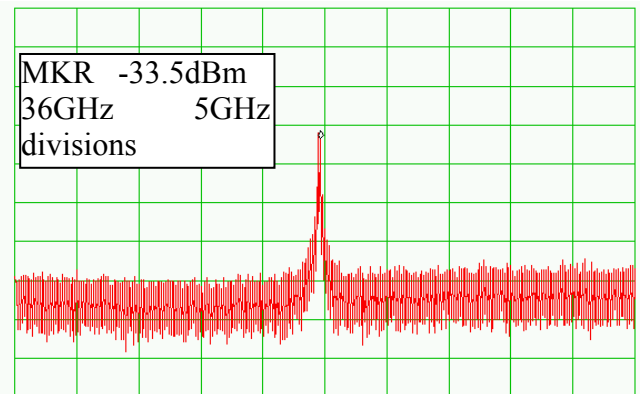


**Figure 7:** Experimental spectrum response of 3 $\mu\text{m}$  fabricated device.

Our devices need to be biased in the range 3.5 – 4.5 V for any oscillations to be seen. Often, the data will show a number of tones. The majority of the signals seen however arise as a consequence of intermodulation in the external mixer. The analyser does however have a signal identification function that enables us to ascertain that any given signal is real. Figure 7 shows a typical frequency response for the 3 micron device showing a strong peak at 36GHz which compares extremely well with the simulated response of this device (section 3.1). Figure 8 shows the spectrum for the highest frequency achieved by us so far (108GHz) in a diode structure.

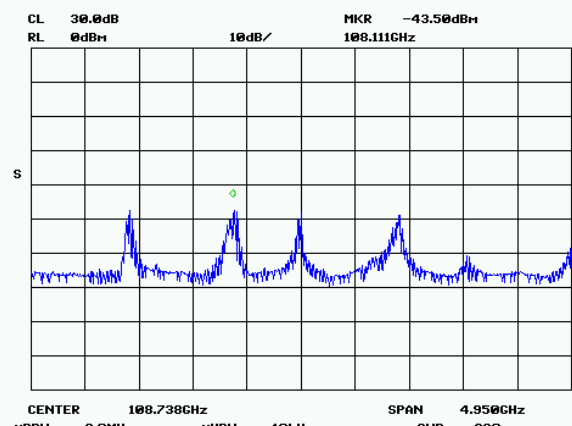


**Figure 8:** Spectrum measured from a typical device. The signal at 108 GHz was confirmed to be the real signal. The others are spurious.

## 4 Conclusions

In this paper, by means of simulations and experimental fabrication, we have shown that HEMT like structures can function as high frequency Gunn oscillators. High accuracy in the fabrication of the surface layers is required so that the surface charge is closely matched by the depletion of the surface layers resulting in very low lateral electric fields in the active regions of the device. Simulations indicate that reasonable powers of about 5% efficiency (typical of Gunn diodes operating in fundamental mode) may be expected of such devices and all of our simulations are in excellent agreement with experiment. The signal power is admittedly small at present and we attribute this to the narrow width of the device, the fact that no on-chip waveguide has yet been employed to facilitate impedance matching from the diode to the 50  $\Omega$  input impedance of the detector.

In conclusion, we have fabricated and demonstrated a range of planar Gunn diode and triode oscillators capable of operating from 35 to 108GHz in a fundamental mode. To the best of our knowledge, this is the highest frequency achieved by a planar Gunn diode using an AlGaAs/GaAs quantum well structure on a GaAs substrate. We believe that planar Gunn diodes have the potential to become a vital component of future millimetre-wave and terahertz systems.

## Acknowledgements

The work reported in this paper was funded by the Electro-Magnetic Remote Sensing (EMRS) Defence Technology Centre, established by the UK Ministry of

Defence and run by a consortium SELEX Sensors and Airborne Systems, Thales Defence, Roke Manor Research and Filtronic.

## References

- 1 M. Takeuchi, A. Higashisaka, and K. Sekido, IEEE Trans. Electron Devices, (corresp.) **ED-19**, 125,(1972).
- 2 Chryssafis A. and Harrington J., IEEE Trans. Electron Devices, **ED-23**, 426, (1976).
- 3 Thim H.W., (1973), US Patent No. 3 740 666.
- 4 Rieder G., Thim R., Kuch R. and Lubke K., (1983), Archiv elektr. Ubertr, 37, p.217.
- 5 Scheib H., Lubke K., Grutzmacher D., Diskus C.G., and Thim H.W, IEEE Trans. On Microwave Theory and Techniques, 37, (1989), p.2093.
- 6 Yamaguchi K., Asai S. and Kodera H., IEEE Trans on Elec. Dev., ED-23, (1976), p.1283.
- 7 Moglestue V., Eur. Trans. Telecommun. Relat. Technol., 1, p.439.
- 8 Dunn G.M., Phillips A. and Topham P.J., Semicond. Sci. and Tech., 16, (2001), p.562.
- 9 Kuang J.B., Tasker P.J., Chen Y.K., Wang G.W., Eastman L.F., Aina O.A., Hier H., and Fathimulla A., Elec. Lett., (1988), 24, p.1571
- 10 X. Hue, B. Boudart and Y. Crosnier, J. Vac Sci. Technology B **16**(5) (1998).
- 11 L. Springer, C. G. Diskus, K. Lubke, A. Stelzer, H. W. Thim, 1997. Proceeding of the 27<sup>th</sup> European, 22-24 September 1997 pages :296-299.